DOI: 10.13009/EUCASS2022-4900

Numerical simulation of Petrea Volubilis falling seed

F. Bajac [1], C. Mendez [2,3], and J. Kurita [4]
[1] Polytechnic School, Universidad Nacional de Asunción, Paraguay
federico.bajac@fpuna.edu.py
[2] School of Aerospace Engineering, Universidad Politécnica de Madrid, Spain
[3] School of Chemistry, Universidad Nacional de Asunción, Paraguay
cmendez@qui.una.py
[4] School of Engineering, Universidad Nacional de Asunción, Paraguay
jkurita@fiuna.edu.py

Abstract

Petrea Volubilis is an evergreen vine species native to central and South America, characterized by having auto rotating seeds. By comparing the calculated drag force that the seed generates at such falling and rotating conditions with the actual seed weight, a CFD simulation can be validated. The characterization of the seed was carried out. Measurements such as the average weight of several samples were conducted. Falling steady-state velocities, as well as rotational speeds, were measured at our experimental setup. The seeds were digitized using a 3D scanner. Since it is assumed a steady-state condition, i.e., terminal velocity, it is expected this drag force results to be similar to the weight. Boundary sensitivity analysis and Mesh sensitivity analysis were also conducted.

1. Introduction

Several authors such as Azuma et al., analysed winged seeds autorotation as they fall from the tree [1], the function of the wing in these seeds is to decelerate their descent and allow greater dispersal by the wind [2].
To better understand the driving force of rotating seeds experimental, and computational analyses were carried out. A non-Multiphysics software was utilized on this analysis. Therefore, in order to find the critical aerodynamic parameters that describe the relationship between the morphological and kinematic characteristics of seeds with autorotation, a series of seed characterization was performed. Mathematical models for optimization of turbine blades based on these seeds were made by several authors [3]. Experimental studies made by Ref. [4] and [5] shows that the autorotation property is independent of the surface area of the wings of the seeds, but is strongly linked to the leading edge: Reduced area just increases the time to reach-steady state but not the autorotation. Ref. [6] also shows that some other parameter such as the pressure difference from about half chord to the trailing edge, can be almost negligible. This observation was made by performing a CFD analysis.
Although these studies were made for a one-wing seed, almost the same principles can be applied on a five-wing seed. Petrea Volubilis is a shrub or liana native to the tropics and subtropics regions [7]. The seed is located at the base of the flower of this shrub, which has five petal. Once the flower matures, it detaches from the branch and falls freely. It is in this process that autorotation is induced, thus reducing the rate of descent of the seed.
This paper offers a numerical study of the properties of the Petrea Volubilies seed. After experimental analysis where the falling steady state velocity and the rotational velocity were found, a CFD analysis is performed to determine the influence of this two parameters in the resulting drag force. The main goal is to validate the simulations with comparing the calculated drag force with the average weight of the seed.

DOI: 10.13009/EUCASS2022-4900

2. Seed Collection, measurement and digitization.

2.1 Collection

The seed samples were taken in the city of Altos, department of Cordillera, Paraguay. The main criteria for harvesting was that the seeds had to be in perfect condition and fully mature, which can be easily identified as the seeds take on a brownish color once they are ripe, in contrast to their original purple color.

Figure 1: Comparison between the ripe seed of a brown color (left) and unripe seed, with its original purple color (right).

2.2 Measurement

The weight of the seeds was obtained using a digital precision balance, with an average result of 41,075 milligram-force or mgf. Once the CFD analysis is done, this average weight value will be compared with the drag force resulting from the calculations.

2.3 Digitization

The surface of the seed had to be prepared by covered it with foot Powder before scanning [8]. This is made in order to have contrast between the background and the actual seed. The digitization was made using a NextEngine 3D scanner [9], with a maximum resolution of 67.000 points/in² [10]. This ensures a reliable model that represents the real seed in both size and texture. The seed must be initially placed facing the scanner, otherwise, if it is placed vertically, the petals confuse the algorithm that builds de digital model and the scan loses accuracy. Scanning is done sequentially by taking multiple images while a rotating plate performs a 360-degree movement. The entire process takes approximately 10 to 30 minutes, depending on the selected resolution.

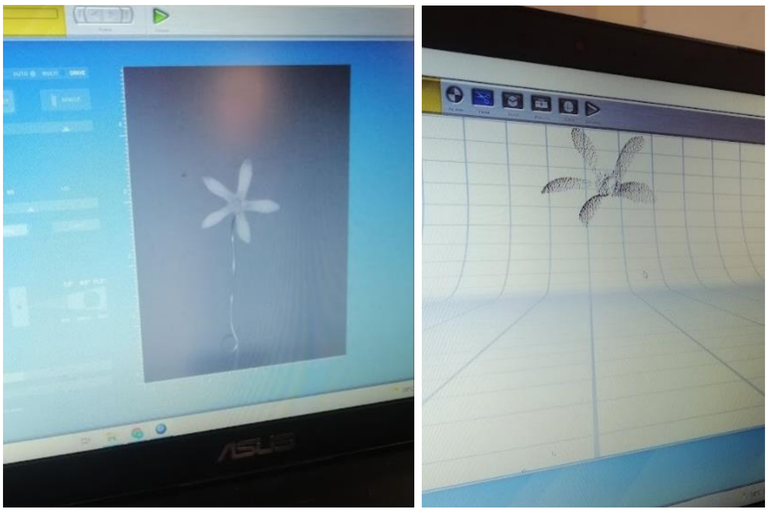

Figure 2: Preview of the seed being supporting by a wire and placed facing the 3D scanner (left). 3D preview of the seed after been scanned (right).

DOI: 10.13009/EUCASS2022-4900

The resulting file was obtained in ".stl" format, so it had to be post-processed to be easily handled in the simulation tools such as SolidWorks software.

Figure 3: Three different views of the resulting scanned seed.

3. Experimental measurement

In order to have the initial conditions that will be set on the CFD analysis, falling steady-state velocities, as well as rotational speeds were measured at our experimental setup.

3.1 Falling steady-state velocity

For the measurement of the Falling Steady-state Velocity, a setup consisting of a positional reference with marks every 3 cm was built, in addition to a cellphone camera at 240 Frames Per Second or FPS, a chronometer and lights.
The seed is dropped freely high above the references, thus ensuring that it reaches steady state and terminal velocity by the time it passes in front of the camera. Using the chronometer, it is possible to find the time differential Δt that elapses since the seed passes from one reference mark to the next. Also knowing that the distance differential Δy between each reference line is 3 cm, and dividing by Δt, the speed of seed fall can be found.

Figure 4: Two instants in which the seed crosses the reference lines separated by 3 cm.

After several tests, it was found that the average rate of fall of the seed in stable state is 0.83 m/s.

3.2 Angular velocity

Angular velocity measurements were made with the camera positioned at the top, facing the ground, a chronometer is positioned at the bottom facing the camera, and the petals are marked to track spin..
Letting the seed fall freely induces the autorotation on it. By the time the seed passes in front of the camera, it will have reached its stable state. An instant of the video is marked and the reference petal is tracked. When the petal returns to the same position, it is said that it has made a complete revolution and the instant is marked again. This finds the time at which the seed makes a complete turn.

DOI: 10.13009/EUCASS2022-4900

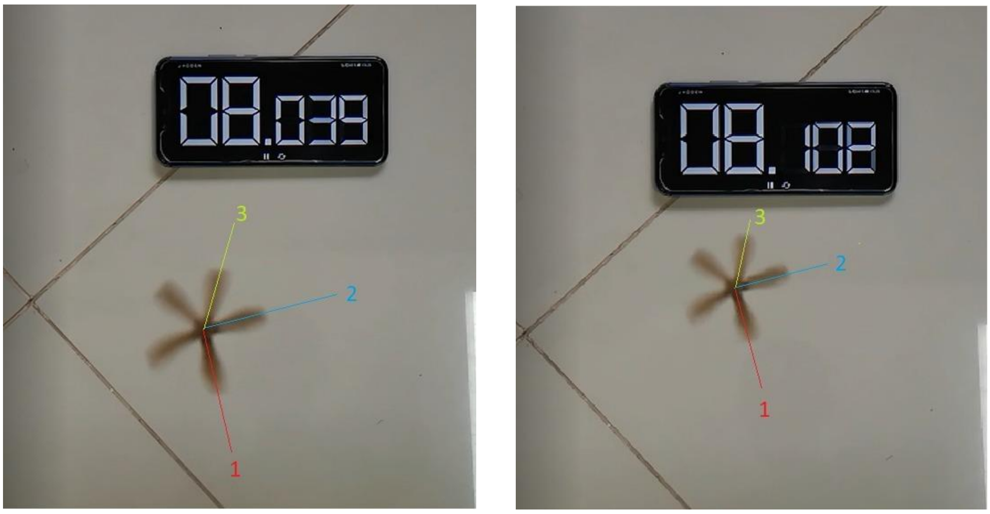

Figure 5: Moment in which petals 1, 2 and 3 return to the same position after having made a complete turn clockwise.

Repeating this test several times, the angular speed was found to be approximately 15.873 revolutions per second or rps.

4. Simulation

Simulations were made on a SolidWorks product called Flow Simulation, which is a widely known tool for CFD solutions.

4.1 Initial and Boundary Conditions

The simulation was set to be an Internal and time-dependent Analysis. The local region (sliding) option for rotations was also selected. Hence, the assembly consisted of three parts. A 100 mm diameter cylinder that acts as a vertical wind tunnel with a 200 mm length, a smaller cylinder of 36 mm of diameter that acts as rotation region and not as a solid, and the 3D model of the seed, which is placed inside of the smaller cylinder.

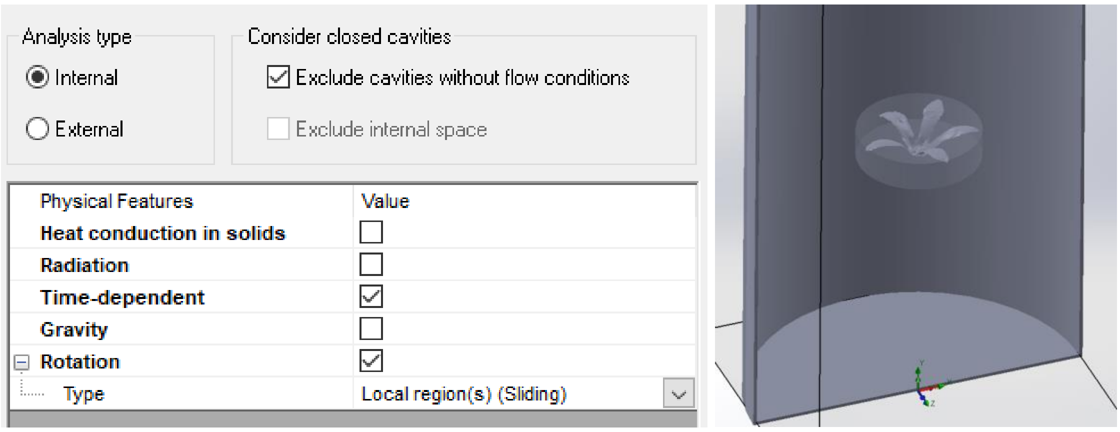

Figure 6: General settings of the Analysis (left). 3D model of the seed placed inside the wind tunnel cylinder and the rotation region cylinder which is concentric with the seed (right).

A summary of the parameters can be found in the table below.

DOI: 10.13009/EUCASS2022-4900

Table 1: Initial condition summary

Analysis type	Internal – Time-Depended
Physical Conditions	Rotational (Local - Sliding)
Fluid	Air
Flow Type	Laminar and Turbulent
Wall condition	Adiabatic Wall
Temperature	293.2 k
Pressure	101325 Pa
Turbulence Intensity	2%
Turbulence length	0.0005 mm

After the creation of the project with the parameter shown above, the data that was experimentally measured previously has to be introduced to the analysis as boundary conditions.
The bottom face of the wind tunnel cylinder was chose as the inlet with a velocity of 0.83 m/s upward, the rest of the internal faces of the bigger cylinder were selected as environmental pressure, and the smaller cylinder as the rotational region, with an angular velocity of negative 15.873 rps (clockwise).

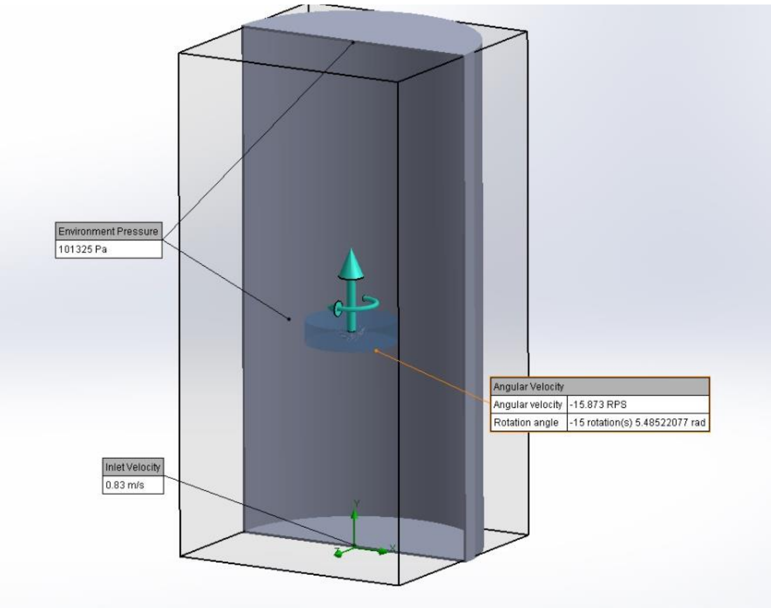

Figure 7: All three boundary conditions experimentally measured previously.

4.2 Meshing and Mesh sensitivity analysis

The mesh sensitivity analysis [11] consists of making a progressive variation of the number of cells in the mesh and observing how the results of the calculations also vary. This is done to obtain an optimal number of cells that is thick enough to have reliable data, but not so thick that the resolution time is not too long.

DOI: 10.13009/EUCASS2022-4900

The SolidWorks automatic mesh control tool was used. The parameters are managed by levels. In addition, a local mesh control was placed on the entire surface of the seed.
The Mesh sensitivity analysis was started with a low level of meshing, resulting in a total of 5 430 cells. The study ended with the level of meshing almost at its maximum, resulting in a total of 127 273 cells. The results of each simulation can be seen in Table 2, and a plot of these results versus the number of cells is shown in Figure 8.

Table 2: Mesh sensitivity analysis results.

N° cells	Inlet Velocity (m/s)	Angular Velocity (rps)	Drag Force (mgf)
127 273	0.83	15.873	43.1
94 428	0.83	15.873	41.4
63 238	0.83	15.873	40.9
55 950	0.83	15.873	40.6
36 660	0.83	15.873	36.9
34 778	0.83	15.873	36.9
29 075	0.83	15.873	30.6
16 668	0.83	15.873	36.4
14 511	0.83	15.873	26.4
12 856	0.83	15.873	28.1
7 787	0.83	15.873	30.1
5 430	0.83	15.873	22.4

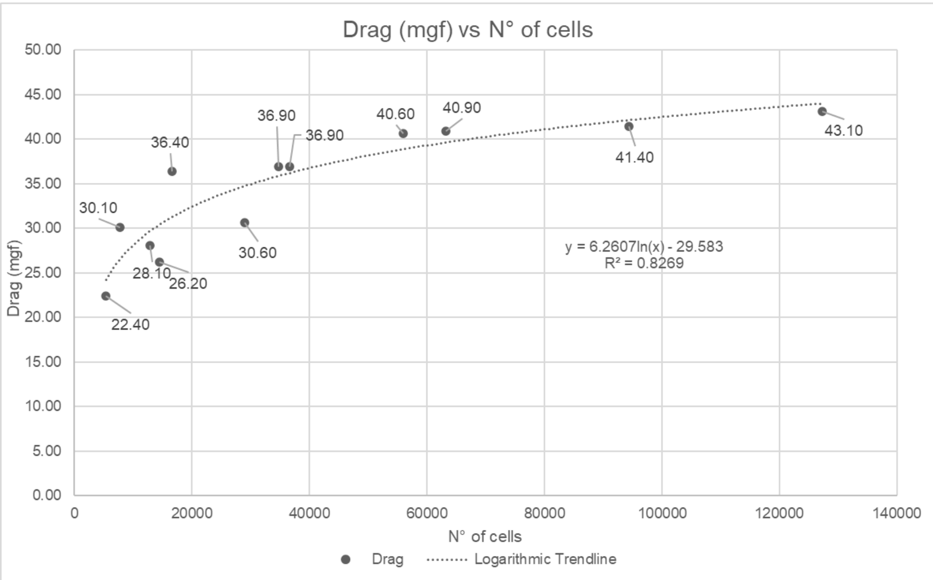

Figure 7: Resulting calculated drag force versus number of cells.

DOI: 10.13009/EUCASS2022-4900

4.3 Boundary Sensitivity analysis

In order to better validate the simulation, a Boundary Sensitivity analysis is also performed. It consists of varying one of the boundary conditions while the others remain constant. In this case, two studies are carried out. The first makes the angular velocity vary in three steps of ±10%. The second makes the input speed vary, also in three steps of ±10%. In order to carry out these studies, the number of cells in the mesh is first fixed. In addition, an intermediate value should be chosen from among the best results of the Meshing sensitivity analysis. For this case, the number of cells selected was 63 238.

4.3.1 Angular Velocity Variation

The first of the Boundary Sensitivity Analysis was with the angular velocity parameter. Its central value is 15 873 rps, so it changes in ±10% steps. A total of six more simulations are done. Their result is shown in the table below.

Table 3: Angular velocity variation for the Boundary Sensitivity Analysis.

N° cells	Inlet Velocity (m/s)	% Variation	Angular Velocity (rps)	Drag Force (mgf)
63 238	0.83	+30%	20.6349	43.9
63 238	0.83	+20%	19.0476	43.1
63 238	0.83	+10%	17.4603	42.1
63 238	0.83	0	15.873	40.9
63 238	0.83	-10%	14.2857	39.5
63 238	0.83	-20%	12.6984	37.9
63 238	0.83	-30%	11.1111	35.9

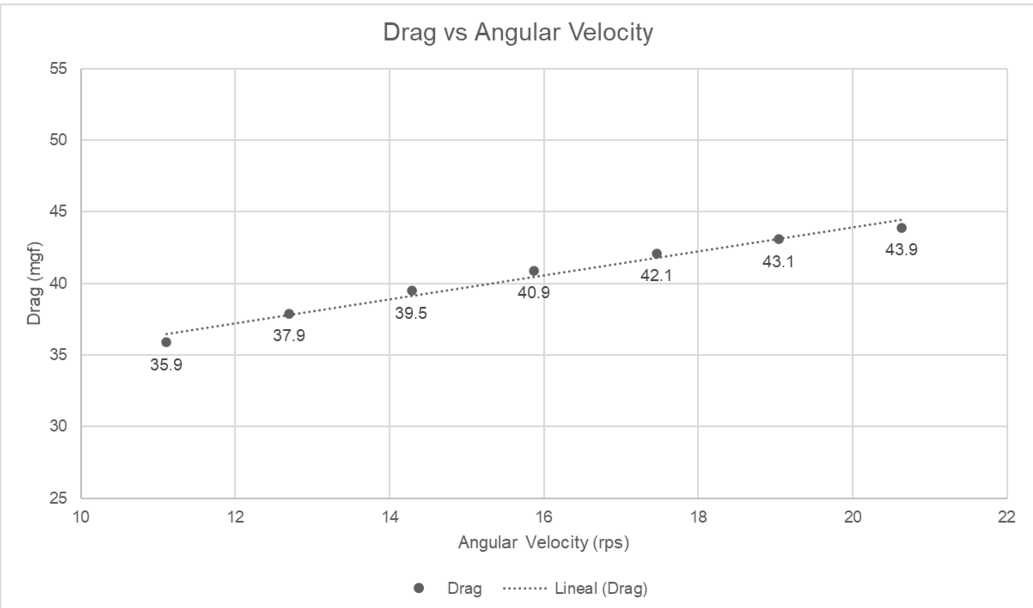

Figure 8: Resulting calculated drag force versus the angular velocity.

DOI: 10.13009/EUCASS2022-4900

4.3.2 Inlet Velocity Variation

The second of the Boundary Sensitivity Analysis was with the inlet velocity parameter. Its central value is 0.83 m/s, so it changes in ±10% steps. A total of six more simulations are done. Their result is shown in the table below.

Table 4: Inlet velocity variation for the Boundary Sensitivity Analysis.

N° cells	% Variation	Inlet Velocity (m/s)	Angular Velocity (rps)	Drag Force (mgf)
63 238	+30%	1.079	15.873	63.1
63 238	+20%	0.996	15.873	55.4
63 238	+10%	0.913	15.873	47.9
63 238	0	0.83	15.873	40.9
63 238	-10%	0.747	15.873	34.2
63 238	-20%	0.664	15.873	27.95
63 238	-30%	0.581	15.873	22.1

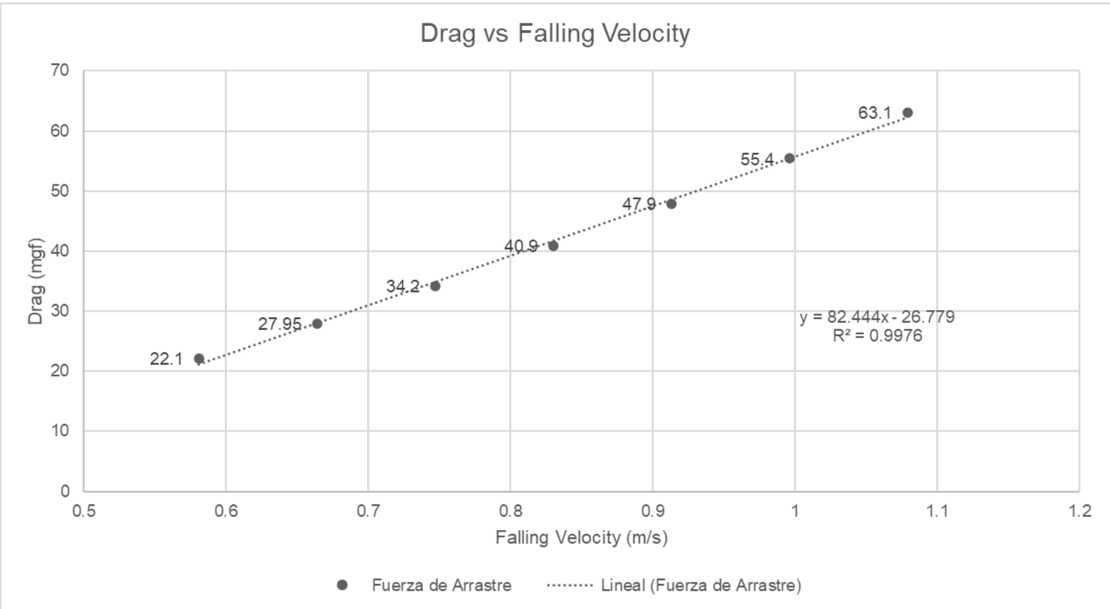

Figure 8: Resulting calculated drag force versus the inlet velocity.

5. Conclusion

The average weight found experimentally was 41.074 mgf. Therefore, to validate this simulation, the calculated drag force should be close to the value of the average weight.
Experimental data of the falling steady-state velocity and rotational speed of the seed were measured. Simulation boundary conditions in this analysis, were set such as characterization was performed.
After performing a mesh sensitivity analysis, it was found that the drag force value converged to 40.9 mgf for a large number of cells. This CFD result differs from the experimental average value by 0.42%.

DOI: 10.13009/EUCASS2022-4900

Boundary conditions sensitivity analysis was conducted in order to verify simulation results reliability. This is because CFD input data were from measurements obtained during seed falling. Values such as the fall rate and rotation rate parameters, were considered for this purpose. These analyzes showed a linear variation of the output drag force as the boundary conditions varying linearly.
For a given falling velocity and rotation speed value 30% less than the central value, the simulated drag force decreases by approximately 12.22%. While for a Falling Velocity value 30% less at a given rotation speed, it is observed that the drag force is down to 46%.
With this it is concluded that the rotation and falling velocity affect the final drag force. The rotation input data was less significant compared to the fall speed.

Acknowledgments

The authors acknowledge Prof. Dr. Marcelo Castier, Dean of the School of Science and Engineering at the Universidad Paraguayo Alemana, and his team, for let us use their 3D scanner and helping us with the 3D modelling of the seeds. Acknowledgments to Abdon Troche for his support, to Blas Vega, because of his willingness to let us use his lab, and to Pablo Sotelo and Pamela Gonzalez of the Biotechnology Department of the Chemistry School – UNA, for let us use their instruments.

References

[1] A. Azuma and K. Yasuda, "Flight performance of rotary seeds," J. theor. Biol, no. 138, pp. 23-53, 1989.
[2] R. D. Lorenz, Spinning flight. Dynamics of frisbees, boomerangs, samaras and skipping stones, Tucson, AZ: Springer, 2006.
[3] I. Lee, "Numerical study of a freely-falling maple seed, Ph.D. thesis," Seoul, 2016.
[4] K. Varshney, S. Chang and Z. J. Wang, "The kinematics of falling maple seeds and the initial," Nonlinearity, vol. 25, pp. C4, C6, 2012. doi:10.1088/0951-7715/25/1/C1.
[5] Ruiz Diaz, Luis O., et al. "Aerodynamic Analysis of Dropping Yvyraro (Pterogyne Nitens) Seed Applied to a Design of a High-Attitude Balloon Descending Speed Reducer." AIAA AVIATION 2022 Forum, 2022. Crossref, https://doi.org/10.2514/6.2022-3465.
[6] J. R. Holden, T. M. Caley and M. G. Turner, "Maple Seed Performance as a Wind Turbine," in 53rd AIAA Aerospace Sciences Meeting, Kissimmee, Florida, 2015. doi:10.2514/6.2015-1304.
[7] Vélez-Gavilán, Jeanine. "Petrea Volubilis (Queen's Wreath)." CABI, 2020. Crossref, https://doi.org/10.1079/isc.39815.20203483496.
[8] University of Minnesota. 3D Scanner User's Manual. NextEngine, 2009, www.mdc.umn.edu/facility/files/electrical/Elec%20Manuals/3D%20Scanner%20User%20Manual.pdf.
[9] "Scanner Accuracy - High Fidelity. Low Price." NextEngine, www.nextengine.com/products/scanner/features/accurate. Accessed 17 June 2022.
[10] "Shapeways." NextEngine, www.nextengine.com/shapeways. Accessed 17 June 2022.
[11] Magomedov, I. A., et al. "Key Steps for Performing Numerical Analysis Utilizing Modern Software Tools." Journal of Physics: Conference Series, vol. 1889, no. 4, 2021, p. 042078. Crossref, https://doi.org/10.1088/1742-6596/1889/4/042078.